ACS OMEGA

http://pubs.acs.org/journal/acsodf

Article

Algebraic Method for Solving Multiple Degenerate Eigenvalues in [*r*]Triangulenes

Jerry Ray Dias*

Cite This: *ACS Omega* 2023, 8, 18332−18338

Read Online

ACCESS | Metrics & More | Article Recommendations

ABSTRACT: An algebraic procedure for overcoming the multiple degeneracy problem in eigenvalue (root) determination of the characteristic polynomial of 3-fold symmetrical molecular graphs is given. This leads to the tabulation of Hückel molecular orbital binding energy (E_π) and eigenvalues (roots) for [2]triangulene to [9]trianguene for the first time. Triangulenes are the smallest possible condensed benzenoid polyradicals.

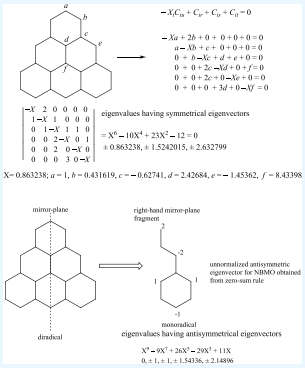

INTRODUCTION

The first synthesis of triangulene was attempted to ascertain whether the hydrocarbon was rendered more stable than is implied by the diradical formula, which was performed by Clar and Stewart before 1952.[1] Subsequently, the synthesis and studies of triangulene derivatives were reported.[2−4] The recent surge in interest in triangulene was brought into focus by the single molecule synthesis of triangulene ([3]triangulene) itself by a tip-assisted approach using a combined scanning tunneling and atomic force microscope.[5] This was followed by single molecule synthesis of [4]triangulene, [5]triangulene, and [7]triangulene.[6−8] Various [*r*]triangulenes have been featured in a number of recent papers.[9−11] Here, *r* is the number of rings along each of the three equilateral edges of the triangulene molecular graph.

In general, triangulenes possess numerous multiple degenerate eigenvalues. Since obtaining the roots (eigenvalues) of characteristic polynomials of molecular graphs with multiple degenerate eigenvalues is challenging by normal factorization procedures, we give an analytical reduction procedure for solving these degenerate eigenvalues in [*r*]triangulenes, which gives greater intuitive insights than the brute force of matrix diagonalization. The Hückel molecular orbital binding energy for [4]triangulene to [9]trianguene is presented for the first time. The consequence of high degeneracy in the frontier orbitals of the [*r*]triangulenes is discussed.

RESULTS AND DISCUSSION

Our approach to circumvent the difficulty of solving multiple degenerate eigenvalues in [*r*]triangulenes involves decomposing their 3-fold molecular graphs into three irreducible subgraphs; two of the three irreducible subgraphs are identical, explaining the double degeneracy. The unique subgraph is the carrier of the unique eigenvalues. The [*r*]triangulenes have vertex-centric (r = 2−3, 5−6, ...) and ring-centric (r = 4, 7, ...) sets; there are two-times as many vertex-centric [*r*]triangulenes as ring-centric ones. The center vertex of these systems occurs in two sets. In one set, the center vertex is starred, and in the other, it is unstarred. To decompose 3-fold molecular graphs composed of fused hexagonal rings, one must distinguish between vertex-centric and ring-centric systems. The total number of carbons in ring-centric [*r*]triangular species is divisible by three ($N_c/3$ = integer), and for the vertex-centric species, it is $(N_c - 1)/3$ = integer. The general formula for [*r*]triangulenes is $C_{r^2+4r+1}H_{1/2(r^2+r)+6}$. It should be noted that the unpaired electrons in [*r*]triangulenes only travel over the starred carbon vertices.

Method of Calculation. Figure 1 gives the irreducible subgraphs for the vertex-centric and ring-centric molecular graphs for [2]−[4]triangulenes. For vertex-centric PAH molecular graphs, the threefold rotational operation defines three equivalent sets of vertices (R, S, and T) and a self-equivalent vertex (v_a) lying on the axis of rotation. To construct

Received: April 12, 2023
Accepted: April 27, 2023
Published: May 9, 2023

https://doi.org/10.1021/acsomega.3c02488
ACS Omega 2023, 8, 18332−18338

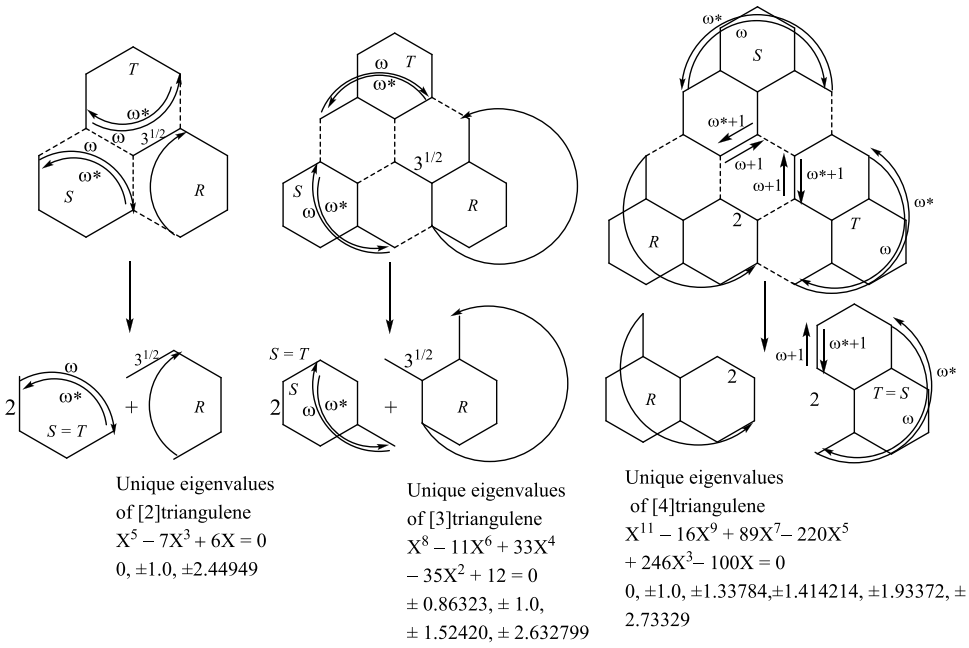

Figure 1. Irreducible subgraphs of [2]−[4]triangulenes. [2]Triangulene and [3]triangulene are vertex-centric molecular graphs, and [4]triangulene is a ring-centric molecular graph.

the unique subgraph G_a, draw the set R together with all the edges connecting the members of the set including additional normal edges for pairs of vertices originally connected to symmetry-equivalent vertices belonging to the adjacent set R in the original molecular graph. The weight of the undirected edge connected to v_a becomes $3^{1/2}$. To construct the remaining two subgraphs G_S and G_T, draw the set S and set T as done for the unique subgraph but without the self-equivalent vertex but instead the additional edges become complex edges of weights ω^* and ω. To illustrate this method, consider Figure 1, which shows the irreducible subgraphs for the vertex-centric molecular graphs of [2]−[3]triangulenes. The additional normal edges in the unique subgraphs (R) are indicated by curved arrows for emphasis, and the complex edges in the two identical subgraphs (S and T) are indicated by opposing pairs of arrows labeled by ω^* and ω.[12,13] The characteristic polynomial with their corresponding eigenvalues listed below the unique irreducible subgraphs was easily determined by the Balasubramanian program for weighted graphs. All unique subgraphs are alternant carbon species. The odd carbon unique subgraphs will have an odd number of zero eigenvalues and the even carbon ones an even number zero eigenvalues. An example of the graph theoretical determination of the characteristic polynomial of one of the irreducible subgraphs with the single complex edge for [3]triangulene that gives one set of the doubly degenerate eigenvalues is given in the upper part of Figure 2.

For ring-centric PAH molecular graphs, the threefold rotational operation defines three equivalent sets of vertices (R, S, and T). To construct the unique irreducible subgraph G_a, draw the set R together with all the edges connecting the members of the set including additional normal edges for pairs of vertices originally connected to symmetry-equivalent vertices belonging to the adjacent set R in the original molecular graph. The edge of R embedded in the central hexagonal ring of the original molecular graph is given the weight two. In construction of the other two irreducible subgraphs G_e, draw the sets of S and T together with all the edges connecting the members of each set

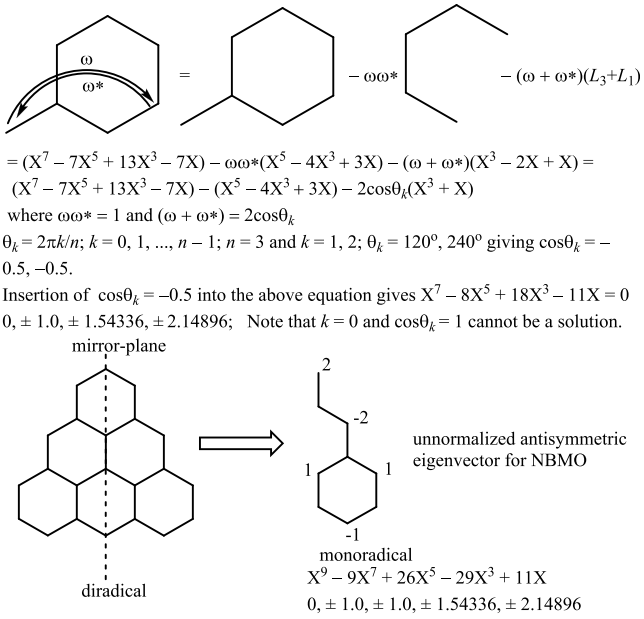

Figure 2. The irreducible subgraph for the doubly degenerate eigenvalues of [3]triangulene and its right-hand mirror-plane fragment give one set of the doubly degenerate eigenvalues except the right-hand fragment that has in addition one unique eigenvalue of ±1.0.

including additional complex ω^* and ω edges for pairs of vertices originally connected to symmetry-equivalent vertices belonging to the adjacent sets S and T in the original molecular graph. The edges of S and T embedded in the central hexagonal ring of the original molecular graph are complex edges of weight of $\omega^* + 1$ and $\omega + 1$.[12,13] This process is illustrated in Figure 1 for [4]triangulene. The characteristic polynomial with their corresponding eigenvalues that are listed below the unique irreducible subgraphs of [4]triangulene was easily determined by the Balasubramanian program for weighted graphs.[14] All the unique irreducible subgraphs can be solved in this way (Figure

https://doi.org/10.1021/acsomega.3c02488
ACS Omega 2023, 8, 18332−18338

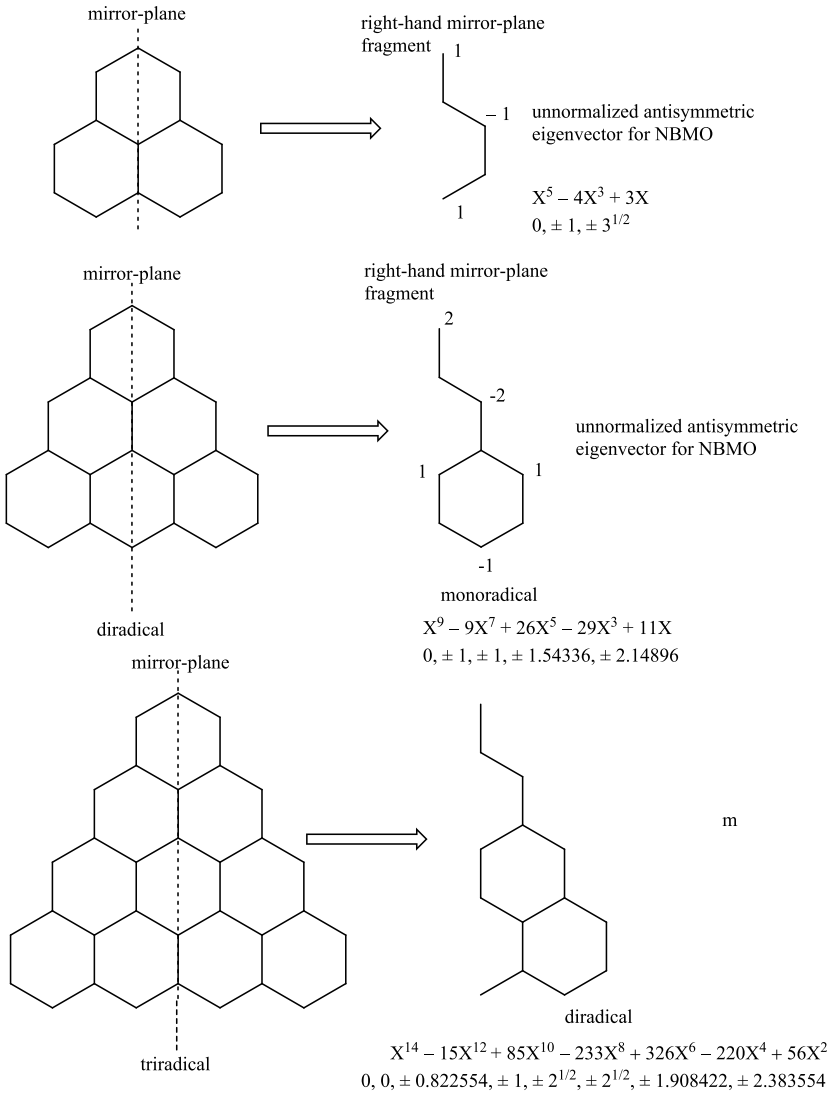

Figure 3. Right-hand mirror-plane fragments of [2]−[4]triangulenes.

1). The graph theoretical determination of the characteristic polynomial of the irreducible subgraphs with multiple complex edges for [5]triangulene and larger triangulenes is far more complicated, and we will now describe our method using mirror-plane fragmentation to circumvent this problem for [*r*]-triangulenes.

Calculation Results. Mirror-plane fragmentation of molecular graphs having twofold or greater symmetry by the McClelland rules[15−17] leads to simplification in determining their characteristic polynomials and eigenvalues. All the right-hand mirror-plane fragments can easily be solved by the Balasubramanian program because they are devoid of complex edges. The right-hand mirror-plane fragment of 3-fold symmetrical molecular graphs always contain one set of its doubly degenerate eigenvalues along with some unique eigenvalues, as shown in the lower part of Figure 2.[18] All the eigenvalues obtained from the right-hand mirror-plane fragments have antisymmetric eigenvectors in regard to this mirror-plane (Figure 3). The unique eigenvalues can be identified by examining the unique eigenvalues determined from the corresponding irreducible subgraphs from the 3-fold decomposition describe above for Figures 1 and 2. Subtracting out these common unique eigenvalues from the eigenvalue set determined for the right-hand mirror-plane fragment and doubling the remaining mirror-plane eigenvalues and adding the unique eigenvalues of the corresponding unique irreducible subgraph will give all the eigenvalues belonging to a given [*r*]triangulene. The right-hand mirror-plane fragments are given in Figure 3 for [2]-, [3]-, and [4]triangulene for comparison with the unique eigenvalues given in Figure 1. In this eigenvalue determination process, it needs to be noted that one should expect at least three eigenvalues of ±1 because of ethene embedding on the three equilateral edges of [*r*]triangulene per the descriptive rules of Hall[12,13] and $r - 1$ zero eigenvalues per the Gordon-Davison peak to valley difference rule and their excised internal structures. Since [*r*]triangulenes are bipartite (alternant) polycyclic conjugated hydrocarbons, they can be maximally starred such that every starred carbon vertex is not adjacent to another starred carbon and every non-starred carbon is likewise not adjacent to another. Thus, the difference between the number of starred carbon vertices and non-starred vertices is also equal to the number zero eigenvalues in [*r*]triangulenes. For [2]triangulene, the zero eigenvalue in the right-hand mirror-plane fragment is identified as the only unique eigenvalue and the other eigenvalues (± 1, $\pm 3^{1/2}$) belong to one set of degenerate eigenvalues. For [3]triangulene, one of the two ±1

https://doi.org/10.1021/acsomega.3c02488
ACS Omega 2023, 8, 18332−18338

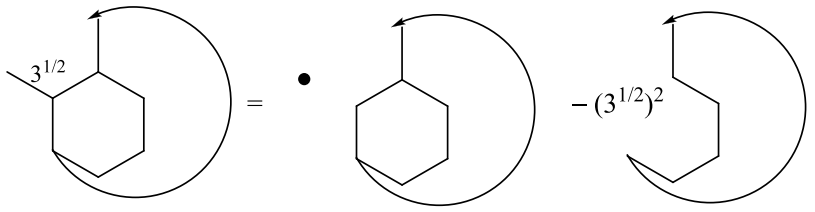

$$= X(X^7 - 8X^5 + 15X^3 - 8X) - 3(X^6 - 6X^4 + 9x^2 - 4) = X^8 - 11X^6 + 33X^4 - 35X^2 + 12$$

Figure 4. Operating on the $3^{1/2}$ weighted edge gives the integer 3, which avoids decimal errors that evolve if $3^{1/2}$ = 1.73205 is used in the Balasubramanian characteristic polynomial program.

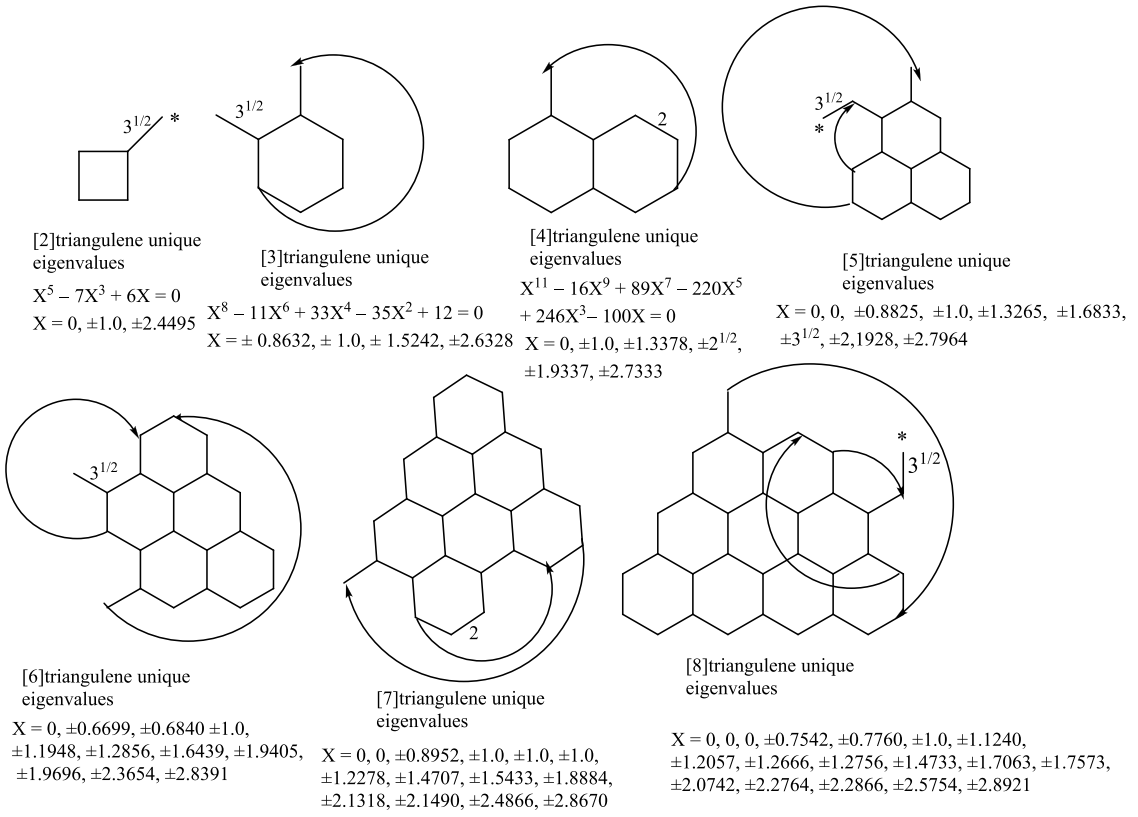

Figure 5. Irreducible subgraphs that give the unique eigenvalues for [2]−[8] triangulenes.

eigenvalues in the right-hand mirror-plane fragment is identified as the unique eigenvalues and the other eigenvalues (0, ±1, ±1.54336, ±2.14896) belong to one set of degenerate eigenvalues. For [4]triangulene, one of the $\pm 2^{1/2}$ eigenvalue in the right-hand mirror-plane fragment is identified as a unique eigenvalue and the other eigenvalues (0, ±0.822554, ±1, $\pm 2^{1/2}$, ±1.908422, ±2.383554) belong to one set of degenerate eigenvalues. Thus, in this comparison of Figures 1 and 3, we were able to determine all the respective eigenvalues for [2]-, [3]-, and [4]triangulenes. At this point, one might inquire why we could not determine the other eigenvalues for the left-hand mirror-plane fragments using the Balasubramanian program. The reason is that left-hand mirror-plane fragments have numerous square root weighted edges, which leads to decimal round off problems in determining their characteristic polynomial roots. Decimal round off problems in determining the characteristic polynomial roots for right-hand mirror-plane fragments of [9]triangulene and larger triangulenes occur. Also, operating on the $3^{1/2}$ weighted edge in the unique vertex-centric irreducible subgraphs gives the integer 3 per Figure 4, which avoids decimal errors that evolve if $3^{1/2}$ = 1.73205 is used in the Balasubramanian characteristic polynomial program.[14] In general, all [r]triangulenes have at least three ±1 eigenvalues and r − 1 zero eigenvalues. As the number of zero eigenvalues increase, we expect that the [r]triangulene will become increasingly more electrically conductive.

Figure 5 summarizes the unique irreducible subgraphs for the [2]−[8]triangulenes including their respective unique eigenvalues. Every third subgraph has a weighted-2 edge and belongs to a ring-centric triangulene. The vertex-centric molecular graphs occur in pairs where the first one has a starred central carbon vertex and second does not. This results in their paired respective irreducible subgraphs having dangling $\sqrt{3}$ weighted edges where the end carbon in the first one is starred and in the second is not. Taking the sum of eigenvalues for the unique irreducible subgraphs [E_π(unique sum)] in Figure 5 and plotting against their corresponding total binding energy [E_π(total)] in Table 1 give a linear equation of E_π(unique sum) = 0.3289E_π(total) + 1.5498 (R^2 = 0.9996). Using this highly correlative equation, one can obtain the total binding energy of

https://doi.org/10.1021/acsomega.3c02488
ACS Omega 2023, 8, 18332−18338

Table 1. List of the Smallest Benzenoids of Each Radical Degree

molecule [no. of rings along each edge] triangulene	formula [radical degree]	number of resonance structures (SC)	E_π, β
benzene ([1]triangulene)	C_6H_6 [0]	2	8.0000
phenalenyl ([2] triangulene)	$C_{13}H_9$ [1]	20	17.8272
[3]triangulene	$C_{22}H_{12}$ [2]	306	30.8098
[4]triangulene	$C_{33}H_{15}$ [3]	7 376	46.9533
[5]triangulene	$C_{46}H_{18}$ [4]	273 956	66.2511
[6]triangulene	$C_{61}H_{21}$ [5]	15 345 156	88.7016
[7]triangulene	$C_{78}H_{24}$ [6]	1 274 990 124	114.3042
[8]triangulene	$C_{97}H_{27}$ [7]	155 024 945 978	143.0562
[9]triangulene	$C_{118}H_{30}$ [8]	27 422 185 371 264	173.8373
[10]triangulene	$C_{141}H_{33}$ [9]	6 981 850 496 603 886	
[11]triangulene	$C_{166}H_{36}$ [10]	2 547 185 424 690 611 836	

even larger [r]triangulenes ($r > 9$) with minimal computational effort.

Table 2 summarizes all the eigenvalues obtained from the irreducible subgraphs (Figure 5) and the right-hand mirror-plane fragments (Figure 6) in HMO β units for [2]triangulenes to [9]triangulene. The eigenvalue distribution displays the following notable correlations. The number of zero eigenvalues increase according to the Gordon-Davison peak to valley difference rule and the difference between the number of starred carbon vertices and non-starred vertices rule for bipartite molecular polyhex graphs. The largest eigenvalues gradually approach the value 3.0 (2.4495 to 2.9092 for [2]- to [9]triangulene), as predicted by the Fröbenius theorem. The eigenvalues of $\pm\sqrt{2} \times 3$ for [4]- and [9]triangulenes are predicted by the embedding of the perimeter by allyl and 3-ethenyl-4-methylenylhexatriene, as shown in Figure 4 of ref 19. The number of eigenvalues of ±1.0 is three for all [r]-triangulenes except [7]triangulene that has two extra ±1.0 eigenvalues as predicted by Hall's descriptive rules due to mixed ethene and pentadienyl embeddings.[12,13] The eigenvalue $\pm\sqrt{3}$ is predicted by pentadienyl embedding of the perimeter of [5]triangulene.

Known Properties. It is known that [3]triangulene is a diradical that exists in a triplet ground state, which arises from the double degeneracy of the HOMO.[4,5,20] Both [4]triangulene

Table 2. HMO Eigenvalue (β) Summary for [2]Triangulene to [9]Triangulene

$C_{13}H_9$	$C_{22}H_{12}$	$C_{33}H_{15}$	$C_{46}H_{18}$	$C_{61}H_{21}$	$C_{78}H_{24}$	$C_{97}H_{27}$	$C_{118}H_{30}$
0.0	0.0 ×2	0.0 x3	0.0 ×4	0.0 ×5	0.0 ×6	0.0 ×7	0.0 ×8
±1.0 ×3	±0.8632	±0.8226 ×2	±0.7484 ×2	±0.6699	±0.6145 ×2	±0.5617 ×2	±0.5157
$\pm\sqrt{3}$ ×2	±1.0 ×3	±1.0 ×3	±0.8825	±0.6840	±0.8176 ×2	±0.7542	±0.5176
±2.4495	±1.5242	±1.3378	±1.0 ×3	±0.8637 ×2	±0.8952	±0.7760	±0.7139 ×2
	±1.5434 ×2	$\pm\sqrt{2}$ ×3	±1.2164 ×2	±1.0 ×3	±1.0 ×5	±0.8780 ×2	±0.8248 ×2
	±2.1489 ×2	±1.9084 ×2	±1.3265	±1.0998 ×2	±1.1345 ×2	±0.9208 ×2	±0.8689 ×2
	±2.6328	±1.9337	±1.3398 ×2	±1.1948	±1.2278	±1.0 ×3	±0.9047
		±2.3836 ×2	±1.6833	±1.2743 ×2	±1.2388 ×2	±1.0657 ×2	±1.0 ×3
		±2.7333	$\pm\sqrt{3}$	±1.2856	±1.3903 ×2	±1.1241	±1.0897 ×2
			±1.7664 ×2	±1.5300 ×2	±1.4707	±1.1990 ×2	±1.1609 ×2
			±2.1549 ×2	±1.6364 ×2	±1.5434	±1.2057	±1.1707
			±2.1928	±1.6439	±1.5480 ×2	±1.2666	±1.1832 ×2
			±2.5301 ×2	±1.9405	±1.7781 ×2	±1.2756	±1.2921 ×2
			±2.7964	±1.9696	±1.8706 ×2	±1.3813 ×2	±1.3399
				±2.0191 ×2	±1.8884	±1.4733	$\pm\sqrt{2}$ ×3
				±2.3270 ×2	±2.1318	±1.4739 ×2	±1.4977
				±2.3654	±2.1490	±1.6301 ×2	±1.5060 ×2
				±2.6287 ×2	±2.2021 ×2	±1.7063	±1.5059
				±2.8391	±.2.4515 ×2	±1.7574	±1.6010 ×2
					±2.4866	±1.7739 ×2	±1.6780 ×2
					±2.6988 ×2	±1.9716 ×2	±1.6851
					±2.8696	±2.0531 ×2	±1.8242 ×2
						±2.0742	±1.8918
						±2.2764	±1.9319
						±2.2866	±1.9552 ×2
						±2.3381 ×2	±2.1239 ×2
						±2.5443 ×2	±2.1962 ×2
						±2.5752	±2.3175
						±2.7506 ×2	±2.3881
						±2.8921	±2.3942
							±2.4418 ×2
							±2.6154 ×2
							±2.6427
							±2.7900 ×2
							±2.9092

https://doi.org/10.1021/acsomega.3c02488
ACS Omega 2023, 8, 18332−18338

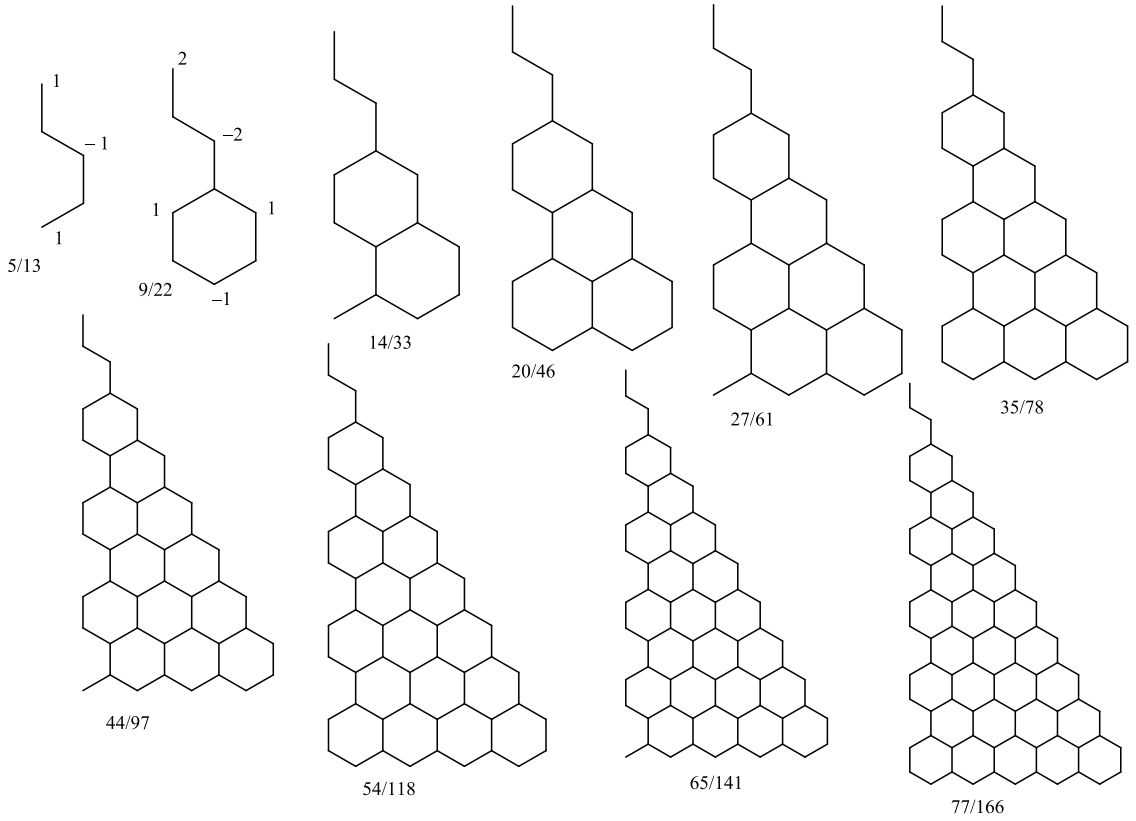

Figure 6. Right-hand mirror-plane fragments of [2]−[11]triangulenes. The first number is the number of carbons of the given fragment, and the second is the number of carbons of the parent.

and [5]triangulene retain their open-shell ground state on an inert Au(111) surface.[6,7] However, based on a combination of density functional theory and scanning tunneling spectroscopy, it is suggested that [7]triangulene results in a closed shell state on Cu(111) with considerable charge transfer.[8] Here, we imagine that the more reactive Cu(111) and the greater unpaired electron density are uniquely operating.

Both the phenalenyl monoradical and [3]triangulene diradical have been extensively studied. A recent review emphasizes various macroscale synthetic approaches to Clar's hydrocarbon ([3]triangulene).[20] In this review, Figure 5 displays the Kekulé structures of [4]triangulene, [5]triangulene, and [7]triangulene that maximizes their sextets with the unpaired electrons located at solo positions. A similar rendition of [10]triangulene can be found in Figure 9 of ref 21. The [*r*]triangulenes with three equilateral edges are the smallest condensed polyradical benzenoids possible. The phenalenyl monoradical and [3]-triangulene diradical are the first members of the respective radical constant-one-isomer series.[22] Circumscribing the $C_{33}H_{15}$ [4]triangulene triradical once gives the $C_{69}H_{21}$ triradical, which is the first-generation member of the unique triradical $\boldsymbol{D}_{3h}$ constant-one-isomer series. The formula of $C_{69}H_{21}$ also corresponds to 12 more monoradical benzenoids that are the first-generation members of the monoradical constant-12-isomer series.[23] Similarly, circumscribing the $C_{46}H_{18}$ [5]-triangulene tetraradical twice gives the $C_{142}H_{30}$ tetraradical, which is the first-generation member of the unique $\boldsymbol{D}_{3h}$ constant-one-isomer series. The formula of $C_{142}H_{30}$ also corresponds to 46 diradical and 86 Kekuléan (nonradical) benzenoid hydrocarbons. The 46 $C_{142}H_{30}$ diradicals are the first-generation members of the diradical $\boldsymbol{D}_{3h}$ constant-46-isomer series, and the sum of 1 + 46 + 86 = 133 is the total number of $C_{142}H_{30}$ benzenoid isomers belonging to the first generation of the constant-133-isomer series. Successive circumscribing of the $C_{61}H_{21}$ [6]triangulene pentaradical as shown in Figure 10 of ref 24 gives $C_{325}H_{45}$ as the first-generation member of the unique pentaradical $\boldsymbol{D}_{3h}$ constant-one-isomer series.[24] This brief synopsis demonstrates the important topological relationships that evolve from the [*r*]triangulenes.

AUTHOR INFORMATION

Corresponding Author

Jerry Ray Dias − *Department of Chemistry, University of Missouri, Kansas City, Missouri 64110-2499, United States*; Email: diasj@umkc.edu

Complete contact information is available at: https://pubs.acs.org/10.1021/acsomega.3c02488

Notes

The author declares no competing financial interest.

ACKNOWLEDGMENTS

Support from the UM Board of Curators for grant K0906077 is appreciated.

REFERENCES

(1) Clar, E.; Stewart. Aromatic Hydrocarbons. LXV. Triangulene Derivatives. *J. Am. Chem. Soc.* **1953**, *75*, 2667−2672.

(2) Allinson, G.; Bushby, R. J.; Pallaud, J.-L. ESR Spectrum of a Stable Triplet π Biradical: Trioxyltriangulene. *J. Am. Chem. Soc.* **1993**, *115*, 2062−2064.

https://doi.org/10.1021/acsomega.3c02488
ACS Omega 2023, 8, 18332−18338

(3) Allinson, G.; Bushby, R. J.; Pallaud, J.-L.; Thornton-Pott, M. Synthesis of a Derivative of Triangulene: the First Non-Kekulé Polynuclear Aromatic. *J. Chem. Soc. Perkin Trans.* **1995**, *1*, 385−390.
(4) Pallaud, J.-L.; Thornton Pott, M.; Inoue, J.; Fukui, K.; Kubo, T.; Nakazawa, S.; Sato, K.; Shiomi, D.; Morita, Y.; Yamamoto, K.; Takui, T.; Nazuhiro, K. The first Detection of a Clar Hydrocarbon, 2,6,10-Tri-tert-Butyltriangulene: A Ground-State Triplet of Non-Kekulé Polynuclear Benzenoid Hydrocarbon. *J. Am. Chem. Soc.* **2001**, *123*, 12702−12703.
(5) Pavlicek, N.; Mistry, Z.; Moll, N.; Meyer, D.; Fox, D. J.; Grass, L. Synthesis and characterization of triangulene. *Nat. Nanotechnol.* **2017**, *12*, 308−311.
(6) Mishra, S.; Beyer, D.; Eimre, K.; Liu, J.; Berger, R.; Groning, O.; Pignedoli, C. A.; Mullen, K.; Fasel, R.; Feng, X.; Ruffieux, P. Synthesis and Characterization of π-Extended Triangulene. *J. Am. Chem. Soc.* **2019**, *141*, 10621−10625.
(7) Su, J.; Telychko, M.; Hu1, P.; Macam, G.; Mutombo, P.; Zhang, H.; Bao, Y.; Cheng, F.; Huang, Z.-Q.; Qiu, Z.; Tan, S. J. R.; Lin, H.; Jelínek, P.; Chuang, F.-C.; Wu, J.; Lu, J. Atomically precise bottom-up synthesis of π-extended [5]triangulene. *Sci. Adv.* **2019**, *5*, No. eaav7717.
(8) Mishra, S.; Xu, K.; Elmre, K.; Komber, H.; Ma, J.; Pignedoli, C. A.; Fasel, R.; Feng, X.; Ruffleux, P. Synthesis and characterization of [7]triangulene. *Nanoscale* **2021**, 1624.
(9) Arikawa, S.; Shimizu, A.; Shiomu, D.; Sato, K.; Shintani, R. Synthesis and Isolation of a Kinetically Stabilized Crystalline Triangulene. *J. Am. Chem. Soc.* **2021**, *143*, 19599−19605.
(10) Zdetsis, A. $4n + 2 = 6n$? A Geometrical Approach to Aromaticity. *J. Phys. Chem. A* **2021**, *125*, 6064−6074.
(11) Toader, A. M.; Buta, C. M.; Frecus, B.; Mischie, A.; Cimpoesu, F. Valence Bond Account of Triangular Polyaromatic Hydrocarbons with Spin: Combining Ab Initio and Phenomenological Approaches. *J. Phys. Chem. C* **2019**, *123*, 6869−6880.
(12) Dias, J. R. Facile Calculations of the Characteristic Polynomial and π-Energy Levels of Molecules Using Chemical Graph Theory. *J. Chem. Educ.* **1987**, *64*, 213−216.
(13) Dias, J.R. *Molecular Orbital Calculations Using Chemical Graph Theory*; Springer-Verlag: Berlin, 1993.
(14) Balasubramanian, K.; Liu, X. Computer Generation of Spectra of Graphs: Application to C60 Clusters and Other Systems. *J. Comput. Chem.* **1988**, *9*, 406−415.
(15) McClelland, B. J. Graphical Method for Factorizing Secular Determinants of Hückel Molecular Orbital Theory. *J.C.S. Faraday Soc. Trans.* **1974**, *70*, 1453−1456.
(16) McClelland, B. J. Eigenvalues of the topological matrix. Splitting of graphs with symmetrical components and alternant graphs. *J. Chem. Soc., Faraday Trans.* **1982**, *78*, 911−916.
(17) McClelland, B. J. On the factorization of Hückel characteristic equations. *Molec. Phys.* **1982**, *45*, 189−190.
(18) Dias, J. R. Characteristic Polynomials and Eigenvalues of Molecular Graphs with a Greater than Twofold Axis of Symmetry. *J. Mol. Struct.: THEOCHEM* **1988**, *165*, 125−148.
(19) Dias, J. R. Structural origin of specific eigenvalues in chemical graphs of planar molecules: Molecular orbital functional groups. *Mol. Phys.* **1995**, *85*, 1043−1060.
(20) Valenta, L.; Jurićek, M. The taming of Clar's hydrocarbon. *Chem. Commun.* **2022**, *58*, 10896−10906.
(21) Dias, J. R. Correlations and topology of triangular benzenoid hydrocarbons: a comparative study of two series representing the least and most stable benzenoid hydrocarbons. *J. Phys. Org. Chem.* **2002**, *15*, 94−102.
(22) Dias, J. R. New General Formulas for Constant-Isomer Series of Polycyclic Benzenoid. *Polycyclic Aromat. Compd.* **2010**, *30*, 1−8.
(23) Dias, J. R. The polyhex/polypent topological paradigm: regularities in isomer numbers and topological properties of select subclasses of benzenoid hydrocarbons and related systems. *Chem. Soc. Rev.* **2010**, *39*, 1913−1924.
(24) Dias, J. R. On the Spectacular Structural Isomorphism between CnHs Monoradical and Cn+sHs+3 Diradical Benzenoid Hydrocarbons: From Reactive Intermediates to Vacancy (Hole) Defects in Graphite. *J. Phys. Chem. A* **2008**, *112*, 3260−3274.

https://doi.org/10.1021/acsomega.3c02488
ACS Omega 2023, 8, 18332−18338